CHEMISTRY
AN ASIAN JOURNAL
ACES
FULL PAPER

DOI: 10.1002/asia.201402467

Development of New Two-Dimensional Small Molecules Based on Benzodifuran for Efficient Organic Solar Cells

Zhengkun Du,[a, b] Yanhua Chen,[a, c] Weichao Chen,[a] Shanlin Qiao,[a] Shuguang Wen,[a] Qian Liu,[a, c] Dangqiang Zhu,[a, b] Mingliang Sun,*[c] and Renqiang Yang*[a, d]

Abstract: A new organic small molecule, DCA3TBDF, with a 2D benzo[1,2-*b*:4,5-*b*′]difuran (BDF) moiety as the central core and octyl cyanoacetate units as the end-capped blocks, was designed and synthesized for solution-processed bulk heterojunction solar cells. DCA3TBDF possesses good solubility in common organic solvents such as toluene, CH_2Cl_2, chlorobenzene, and $CHCl_3$ and good thermal stability with an onset decomposition temperature with 5% weight-loss occurring at 361 °C. The DCA3TBDF thin film showed a broad absorption at $\lambda = 320$–700 nm and high crystallinity. Small-molecule organic solar cells based on DCA3TBDF and [6,6]-phenyl-C_{61}-butyric acid methyl ester demonstrated promising power conversion efficiency with a high fill factor under the illumination of AM 1.5G (100 mW cm^{-2}).

Keywords: benzodifuran · donor–acceptor systems · heterocycles · organic electronics · small molecules

Introduction

In the past decade, organic solar cells (OSCs) have attracted much attention owing to their unique advantages, which include their low fabrication cost, their light weight, and their good mechanical flexibility.[1–5] The introduction of low band-gap conjugated polymers has led to tremendous progress in polymer solar cells (PSCs), and promising power conversion efficiencies (PCEs) of over 9% have been achieved.[6] More recently, solution-processed OSCs based on conjugated small molecules have been developed rapidly because of their definite chemical structure, easy purification, and good synthetic reproducibility.[7–13] Small-molecule organic solar cells (SMOSCs) based on planar linear acceptor–donor–acceptor (A-D-A) type molecules have achieved PCEs over 8%,[8,12] which is very close to the highest PCE of 9.2% reported for PSCs.[6] So far, this relatively low PCE is still a bottleneck in the commercial application of solution-processed SMOSCs. Hence, new low band-gap small molecules need to be designed and synthesized to improve device performance.

To obtain ideal small-molecule donor materials for high-performance OSCs, the synthesis of low band-gap small molecules containing electron-donating groups and electron-withdrawing groups has become a widely used strategy over the past few years.[8,10,12] Among the variety of developed electron-donating materials for SMOSCs, heterocyclic molecules with planar structures have received considerable attention. Recently, benzo[1,2-*b*:4,5-*b*′]dithiophene (BDT) has emerged as a promising electron-donating material for photovoltaic applications owing to its relatively convenient modification and planar conjugated structure, which can enhance π–π stacking in the solid state and enhance electron delocalization.[14–19] To date, SMOSCs based on BDT derivatives have achieved PCEs over 8%.[12] Although the structure of benzo[1,2-*b*:4,5-*b*′]difuran (BDF) is similar to that of BDT, the oxygen atom possesses a smaller diameter and higher electronegativity than a sulfur atom,[20–23] which may result in good packing of BDF-based molecular backbones. Polymers based on BDF have achieved promising PCEs. Hou et al. reported an alternating 2D copolymer of BDF and thieno[3,4-*b*]thiophene (TT), namely, PBDFTT-CF-T, as a donor material and obtained a high PCE of over 6%.[24] However, small molecules with a BDF moiety as the building block for solution-processed OSCs have not been report-

[a] Z. Du, Y. Chen, Dr. W. Chen, Dr. S. Qiao, Dr. S. Wen, Q. Liu, D. Zhu, Prof. R. Yang
CAS Key Laboratory of Bio-based Materials
Qingdao Institute of Bioenergy and Bioprocess Technology
Chinese Academy of Sciences
Qingdao 266101 (China)
Fax: (+86) 532-80662778
E-mail: yangrq@qibebt.ac.cn

[b] Z. Du, D. Zhu
University of Chinese Academy of Sciences
Beijing 100049 (China)

[c] Y. Chen, Q. Liu, Prof. M. Sun
Institute of Materials Science and Engineering
Ocean University of China
Qingdao 266100 (China)
E-mail: mlsun@ouc.edu.cn

[d] Prof. R. Yang
Institute of Polymer Optoelectronic Materials and Devices
State Key Laboratory of Luminescent Materials and Devices
South China University of Technology
Guangzhou 510640 (China)

Supporting information for this article is available on the WWW under http://dx.doi.org/10.1002/asia.201402467.

ed so far. Therefore, the development of BDF-based small molecules may be a strategic choice for solution-processed SMOSCs.

Alkyl cyanoacetates have a simple conjugated structure and strong electron-withdrawing ability.[12] In most cases, not only does the introduction of an alkyl cyanoacetate effectively regulate the energy levels of the highest occupied molecular orbital (HOMO) and lowest unoccupied molecular orbital (LUMO) but it also improves the solubility of the targeted molecules. According to the literature, the alkyl cyanoacetate group is a widely used acceptor for constructing high-performance SMOSCs.[7,9,12]

Considering the above discussions, the investigation of BDF-based small molecules with an alkyl cyanoacetate group as an electron acceptor should be a new donor material for the development of SMOSCs. In this work, we successfully synthesized a novel 2D organic small molecule, DCA3TBDF (Scheme 1), based on 4,8-bis[5-(2-ethylhexyl)thiophen-2-yl]benzo[1,2-*b*:4,5-*b*′]difuran as the central core with octyl cyanoacetate units as the end-capped blocks. DCA3TBDF possesses good solubility in common organic solvents, such as toluene, chlorobenzene, CH_2Cl_2, and $CHCl_3$. It also shows high crystallinity in the DCA3TBDF/$PC_{61}BM$ blend ($PC_{61}BM$ = [6,6]-phenyl-C_{61}-butyric acid methyl ester). The SMOSC based on DCA3TBDF/$PC_{61}BM$ exhibits a PCE of 4.49% with an open-circuit voltage (V_{oc}) of 0.90 V, a short-circuit current density (J_{sc}) of 7.32 mA cm^{-2}, and a high fill factor (FF) of 67.97%.

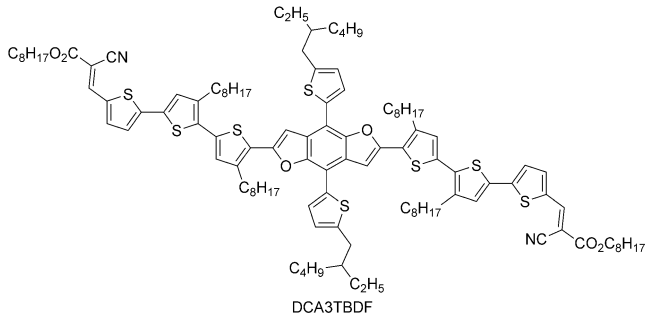

Scheme 1. Molecular structure of DCA3TBDF.

Results and Discussion

Synthesis and Characterization

The detailed synthetic route to DCA3TBDF is given in Scheme 2. The key intermediate, 5″-bromo-4′,4″-dioctyl-2,2′:5′,2″-trithiophene-5-carbaldehyde (**5**), was synthesized through a four-step reaction from 5-bromothiophene-2-carbaldehyde (**1**) by using Stille coupling and bromination reactions. BDF-containing dicarbaldehyde precursor **7** was synthesized by a [$Pd(PPh_3)_4$]-catalyzed Stille coupling reaction between **5** and 2,6-bis(trimethyltin)-4,8-bis[5-(2-ethylhexyl)thiophen-2yl]benzo[1,2-*b*:4,5-*b*′]difuran (**6**) in refluxing toluene under argon protection for 36 h. The target DCA3TBDF small molecule was obtained through Knoevenagel condensation of intermediate **7** with octyl cyanoacetate by using triethylamine as the catalyst in anhydrous $CHCl_3$ for 40 h at room temperature. The structures of all intermediates were verified by NMR spectroscopy. The molecular structure and purity of DCA3TBDF was confirmed by ^{1}H NMR spectroscopy, elemental analysis, and high-resolution mass spectrometry. At relatively low temperatures (40–80 °C), the compound shows good solubility in common organic solvents such as toluene, CH_2Cl_2, *o*-chlorobenzene (*o*-DCB), $CHCl_3$, and trichlorobenzene (TCB).

Thermal Stability

Thermal stability of the small molecule is very important for fabrication of its photovoltaic device. As shown in Figure 1, thermogravimetric analysis (TGA) of DCA3TBDF indicates good thermal stability; the onset decomposition temperature (T_d) with 5% weight loss occurs at 361 °C under a N_2 atmosphere. Such high thermal stability could prevent the deformation of the morphology of a DCA3TBDF film and also prevent the degradation of the small-molecular active layer under applied solution-processed SMOSCs.

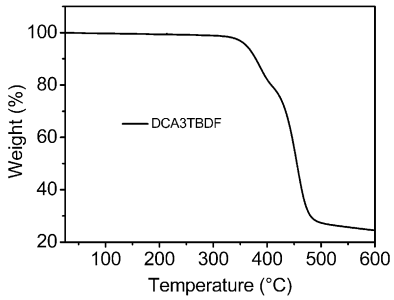

Figure 1. TGA curve of DCA3TBDF at a heating rate of 10 °C min^{-1} under a nitrogen atmosphere.

Optical Properties

The normalized UV/Vis absorption spectra of DCA3TBDF in diluted $CHCl_3$ solution and in the film are shown in Figure 2. In solution, DCA3TBDF displays an absorption band at λ = 320–625 nm and a maximum absorption band at λ = 520 nm. As a film, DCA3TBDF shows two absorption bands at λ = 582 and 635 nm. The long wavelength absorption is mainly caused by the strong D-A charge-transfer state.[19] The absorption of DCA3TBDF in the solid state is strongly redshifted and broader than that in solution, which indicates that the extended 2D BDF planar system of DCA3TBDF is beneficial in promoting π–π stacking interactions.[24–26] The optical band gap calculated from the absorption edge (690 nm) of the thin film is approximately 1.80 eV.

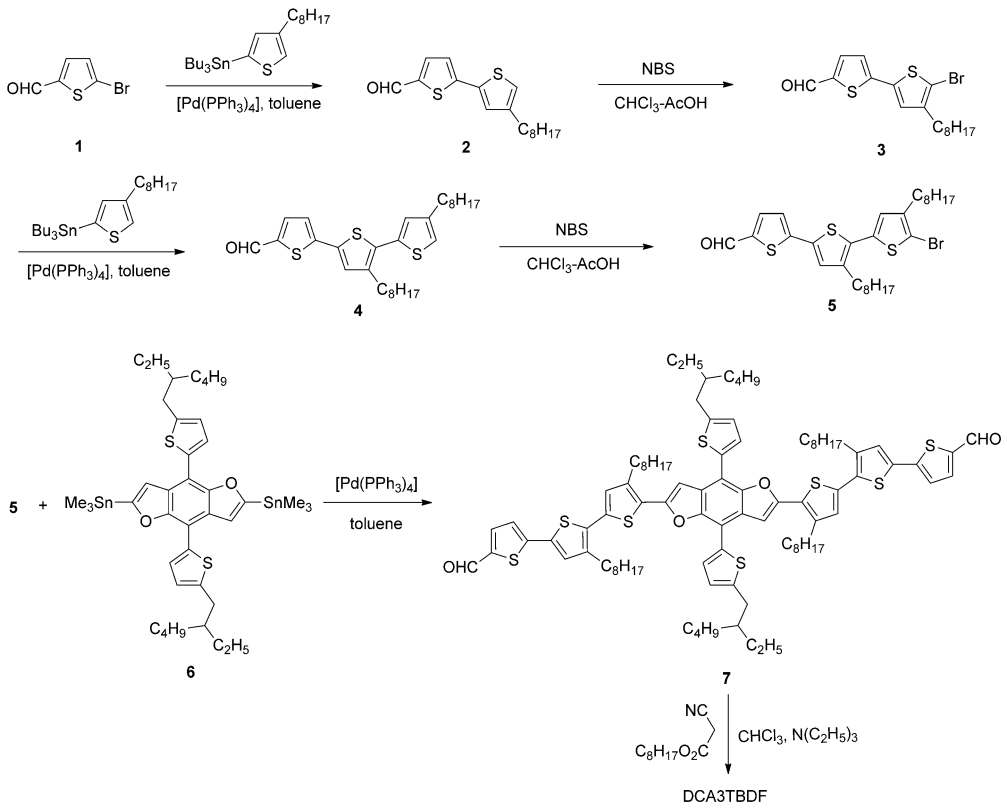

Scheme 2. Synthetic route to DCA3TBDF. NBS = *N*-bromosuccinimide.

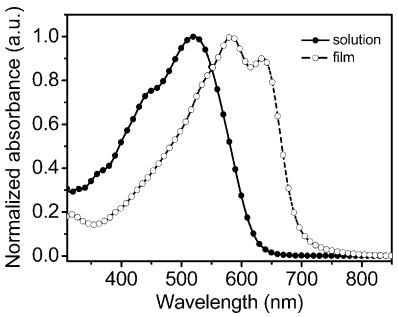

Figure 2. UV/Vis absorption spectra of DCA3TBDF in dilute $CHCl_3$ solution and in thin film.

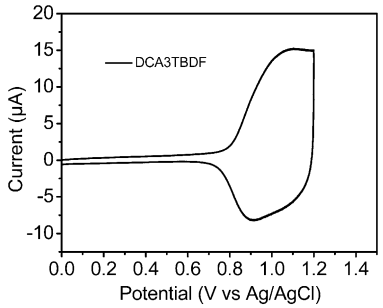

Figure 3. Cyclic voltammogram of a DCA3TBDF film casting on a platinum disk in 0.1 M Bu_4NPF_6/CH_3CN solution at a scan rate of 100 mV s^{-1}.

Electrochemical Properties

The electrochemical properties of DCA3TBDF were investigated by cyclic voltammetry by using a platinum working electrode in 0.1 M Bu_4NPF_6/CH_3CN solution with a scan rate of 100 mV s^{-1}. The onset potential of the oxidation wave of DCA3TBDF was 0.80 V versus Ag/AgCl (Figure 3), which corresponds to a HOMO energy level of −5.12 eV. As is well known, V_{oc} is mainly dependent on the difference between the energy level of the HOMO of the donor and the energy level of the LUMO of the acceptor (usually fullerene derivatives as the acceptor).[13] DCA3TBDF possesses a low-lying HOMO energy level because of the strong electron-accepting ability of the alkyl cyanoacetate unit and the 2D conjugated substituted side chain. Thus, high values of V_{oc} for SMOSCs based on DCA3TBDF and $PC_{61}BM$ could be expected. The LUMO energy level was determined to be approximately −3.32 eV by using its HOMO energy level and the optical band gap. The calculated LUMO energy level of DCA3TBDF is approximately 0.88 eV above the LUMO level (−4.2 eV) of $PC_{61}BM$ as an n-type electron acceptor, which generates a large driving force for the transfer and separation of photogenerated charge carriers in the D-A interface.[3]

Photovoltaic Properties

The photovoltaic properties of DCA3TBDF were investigated with the conventional device structure of ITO/PEDOT:PSS/DCA3TBDF:$PC_{61}BM$/Ca/Al [ITO = indium tin oxide, PEDOT:PSS = poly(3,4-ethylenedioxythiophene) polystyrene sulfonate]. Details of the fabrication and measurements of the device are described in the Experimental Section. The corresponding characteristics of the resulting devices are summarized in Table 1. First, different weight ratios of DCA3TBDF and $PC_{61}BM$ (1:1, 2:1, and 3:1) were investigated to optimize the performance of the device. With increasing D/A ratio in the active layer, the best performance was achieved with DCA3TBDF/$PC_{61}BM$ = 2:1, which reached a PCE of 3.84% with V_{oc} = 0.90 V, J_{sc} = 6.54 mA cm^{-2}, and FF = 65.25% without annealing. If the D/A blend ratio was increased to 3:1, the PCE of the SMOSC was reduced markedly to 1.47% as a result of a reduction in the values of J_{sc} and FF.

Table 1. The photovoltaic performance of SMOSCs based on DCA3TBDF/$PC_{61}BM$ (D/A) with different blend ratios.

Donor/acceptor (D/A)	Annealing [°C][a]	V_{oc} [V]	J_{sc} [mA cm^{-2}]	FF [%]	PCE [%]
1:1	no	0.87	5.76	64.39	3.23
2:1	no	0.90	6.54	65.25	3.84
3:1	no	0.90	2.71	60.29	1.47
2:1	50	0.89	6.70	66.15	4.14
2:1	70	0.90	7.32	67.97	4.49
2:1	90	0.89	7.25	64.86	4.20

[a] Thermal annealing for 10 min.

To further improve the photovoltaic performance of SMOSCs based on DCA3TBDF/$PC_{61}BM$, thermal annealing at different temperatures was employed. By increasing the thermal annealing temperature, the values of J_{sc} and FF of the device first increased and then decreased noticeably. After thermal annealing at 70°C, the optimized device performance was obtained at a blend ration of 2:1, with a PCE of 4.49%, V_{oc} = 0.90 V, J_{sc} = 7.32 mA cm^{-2}, and FF = 67.97%. The absorption intensity of the DCA3TBDF/$PC_{61}BM$ blend film was enhanced by increasing the thermal annealing temperature (see Figure S2), which was thought to be the main reason for the increased value of J_{sc} for the devices. The high value of FF may be ascribed to high crystallinity and high carrier mobility of DCA3TBDF in the film.[27] Notably, all the devices exhibited high V_{oc} values of 0.87–0.90 V because of the low-lying energy level of the HOMO of DCA3TBDF.[28]

The current density versus voltage (J–V) curves of the device with a ratio of 2:1 before and after thermal annealing at 70°C and the corresponding external quantum efficiency (EQE) curves are shown in Figure 4. The EQE curves of the optimized device covered a broad wavelength range from 320 to 700 nm with a maximum EQE value of 43% at 550 nm. The shape of the EQE curve for the DCA3TBDF-based SMOSCs is similar to that of its absorption spectra as a thin film. This result demonstrates that most of the absorbed sunlight of DCA3TBDF-based devices contributes to the generation of the photocurrent.[17] The higher EQE value for DCA3TBDF-based OSCs after thermal annealing at 70°C results in an increased J_{sc} value, and this is in agreement with the J–V measurements. The value of J_{sc} (7.30 mA cm^{-2}) calculated from the EQE spectra is consistent with that measured from the J–V curve (7.32 mA cm^{-2}).

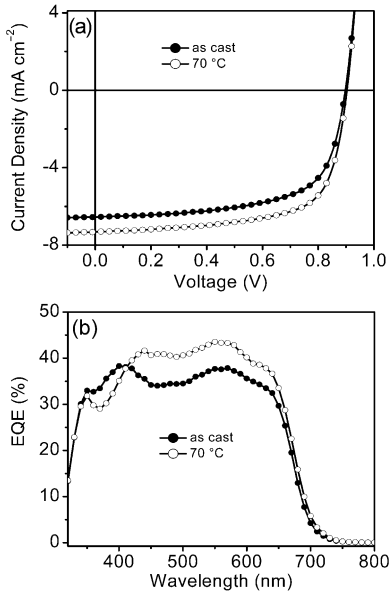

Figure 4. a) J–V characteristics and b) EQE curves of SMOSCs based on DCA3TBDF/$PC_{61}BM$ (2:1 w/w) after thermal annealing at 70°C.

X-ray Analysis

Although DCA3TBDF itself possesses eight alkyl side chains, its solubility in chloroform solution was not good at room temperature. This indicates that DCA3TBDF undergoes strong self-aggregation because of the influence of the BDF unit, which is favorable for ordered arrangement in the solid state. The crystallinity of the DCA3TBDF/$PC_{61}BM$ thin film before and after thermal annealing at 70°C was investigated by X-ray diffraction (XRD) (Figure 5). The film exhibits a narrow (100) reflection peak at 2θ = 4.04°, which

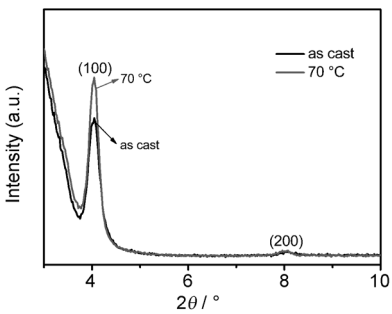

Figure 5. XRD pattern of the DCA3TBDF/$PC_{61}BM$ thin film before and after thermal annealing at 70°C.

corresponds to an interlayer spacing of 21.9 Å. This spacing value is the distance between the planes of the main conjugated backbone of DCA3TBDF separated by the alkyl side chains.[16] The second-order diffraction peak (200) at $2\theta = 8.08°$, corresponding to a d_{200} spacing value of 10.9 Å, was also observed, and this is indicative of the high crystallinity of the DCA3TBDF thin film. The higher crystallinity of the film after thermal annealing at 70 °C could benefit the transport and collection of charge carriers, which may be an important contributor to the high values of J_{sc} and FF for the devices after annealing.

Hole Mobility

Hole mobility is another important factor for small molecules owing its direct influence on charge transport. High hole mobility could guarantee effective charge carrier transport to the electrodes and reduce the photocurrent loss in photovoltaic devices. The hole mobility of DCA3TBDF was measured by space-charge limit current (SCLC)[29–31] theory with a device structure of ITO/PEDOT:PSS/DCA3TBDF:PC_{61}BM/Au. The SCLC is described by [Eq. (1)]:[31]

$$J_{SCLC} = \frac{9}{8}\varepsilon_0\varepsilon_r\mu_h\frac{V^2}{L^3} \quad (1)$$

in which J stands for current density, ε_0 is the permittivity of free space, ε_r is the relative dielectric constant of the transport medium, μ_h is the hole mobility, V is the internal potential in the device, and L is the thickness of the active layer. The internal potential V is obtained by subtracting the built-in voltage (V_{bi}) and the voltage drop (V_s) from the series resistance of the substrate from the applied voltage (V_{appl}) according to Equation (2):

$$V = V_{appl} - V_{bi} - V_s \quad (2)$$

As shown in Figure 6, according to Equation (1), the hole mobility of DCA3TBDF before and after thermal annealing at 70 °C was calculated to be 1.0×10^{-4} and 2.3×10^{-4} $cm^2V^{-1}s^{-1}$, respectively. Under the same measurement conditions, the hole mobility of DCA3TBDF was enhanced mainly because of improved intermolecular interactions and ordered alignment of the blend film after thermal annealing. The high mobility would benefit exciton separation and the transport and collection of the charge carrier.[32] Therefore, the values of J_{sc} and FF were higher for the device after thermal annealing than for the device as cast.

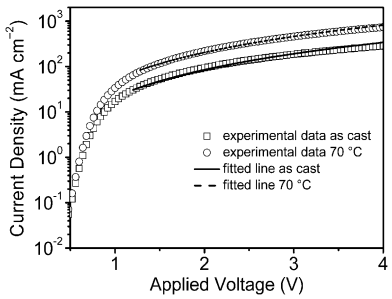

Figure 6. The *J–V* curves of the ITO/PEDOT:PSS/DCA3TBDF:PC_{61}BM (100 nm)/Au diodes before and after thermal annealing at 70 °C. The symbols are experimental data for the transport of holes, and the solid line is fitted according to the space-charge-limited-current model.

Morphology

The morphology of the active layer is important for efficient solution-processed SMOSCs, because effective phase separation is very helpful for exciton separation and carrier transport and collection.[33,34] To further understand the relationship between the morphology of the film and the performance of the device, the morphology of the DCA3TBDF/PC_{61}BM blend film before and after thermal annealing was investigated by using tapping-mode atomic force microscopy (AFM). As shown in Figure 7, the pristine film of the DCA3TBDF/PC_{61}BM blend has a root-mean-square (RMS) roughness of 12 nm, and the film after thermal annealing exhibits a RMS roughness of 12.5 nm, which implies a relatively high level of self-organization in the active layer.[32] Owing to the high crystallinity of DCA3TBDF, strong phase aggregation in the thin film is found, which leads to the relatively low value of J_{sc} for the device.

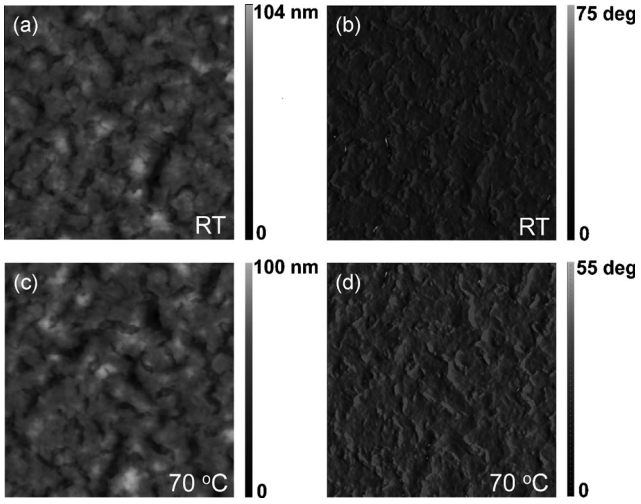

Figure 7. Tapping-mode AFM height (a,c) and phase (b,d) images (4× 4 μm) of DCA3TBDF/PC_{61}BM (2:1 w/w) blend film before (a,b) and after (c,d) thermal annealing at 70 °C.

Conclusions

In conclusion, a new D-A 2D small molecule, DCA3TBDF, based on benzo[1,2-*b*:4,5-*b*′]difuran was designed and synthesized. DCA3TBDF exhibited good thermal stability and a HOMO energy level of −5.12 eV. The X-ray diffraction pattern of DCA3TBDF showed that it exhibited ordered

crystallinity after thermal annealing. A small-molecule organic solar cell device based on DCA3TBDF and $PC_{61}BM$ was prepared and it showed a power conversion efficiency of 4.49% with a high fill factor (67.97%) after thermal annealing at only 70°C. The results indicate that the benzo[1,2-*b*:4,5-*b*′]difuran unit may be a promising electron-donor building block for solution-processed SMOSCs.

Experimental Section

Materials

All starting materials and reagents were purchased from commercial sources and were used without further purification, unless otherwise mentioned. Toluene was dried with sodium by using benzophenone as an indicator. $CHCl_3$ and CH_2Cl_2 were distilled from calcium hydride.

Measurements and characterization

NMR spectra were measured in $CDCl_3$ with a Bruker Advance III 600 spectrometer with tetramethylsilane ($\delta = 0$ ppm) as an internal standard. High-resolution mass spectra were recorded under the atmospheric pressure chemical ionization mode with a Bruker Maxis UHR TOF spectrometer. UV/Vis absorption spectra were obtained with a Hitachi U-4100 spectrophotometer. The surface roughness and morphology of the thin films were characterized by atomic force microscopy (AFM) with an Agilent 5400. The structure of the films was performed with grazing incidence X-ray diffraction (GIXRD, Bruker D8 ADVANCE). Xyclic voltammetry (CV) measurements were taken with a CHI660D electrochemical workstation in 0.1 M tetrabutylammonium phosphorus hexafluoride (Bu_4NPF_6)/acetonitrile solution at a scan rate of 100 mV s^{-1} by using a platinum wire as the counter electrode, a Ag/AgCl electrode as the reference electrode, and a platinum working electrode coated with DCA3TBDF. Ferrocene/ferrocenium (Fc/Fc^+) was used as the internal standard (the energy level of Fc/Fc^+ is −4.8 V under vacuum), and the formal potential of Fc/Fc^+ was 0.38 V vs. an Ag/AgCl electrode.

Fabrication and characterization of the SMOSCs

The bulk heterojunction SMOSCs based on DCA3TBDF were fabricated with a structure of ITO/PEDOT:PSS/DCA3TBDF:$PC_{61}BM$/Ca/Al by using the conventional solution spin-coating process. The ITO-coated glass substrates were cleaned by sequential ultrasonic treatment in detergent, deionized water, acetone, and isopropyl alcohol for 20 min and subsequently oxygen plasma treatment was made for 10 min as the final step. Then, a thin layer of PEDOT:PSS was spin coated onto the ITO surface with a thickness of approximately 40 nm. After baking at 150°C for 25 min, the substrates were transferred into a glove box. Subsequently, the active layer was spin coated in different blend ratios of DCA3TBDF and $PC_{61}BM$ in $CHCl_3$ solution at 1500 rpm for 20 s. Finally, a 10 nm Ca layer and a 100 nm Al layer were successively deposited onto the active layer under high vacuum ($< 2.5 \times 10^{-4}$ Pa). Thermal annealing was performed by placing the completed devices on a digitally controlled hotplate at 70°C in an argon-filled glove box.

The current density–voltage (*J*–*V*) characteristics of the devices were measured with a Keithley 2420 source measurement unit under simulated 100 mW cm^{-2} (AM1.5 G) irradiation from a Newport solar simulator. Light intensity was calibrated with a standard silicon solar cell. The external quantum efficiencies were analyzed by using a certified Newport incident photon conversion efficiency measurement system.

Synthesis

All coupling reactions were conducted under an argon atmosphere. 2-(Tributylstannyl)-4-octylthiophen and 2,6-bis(trimethyltin)-4,8-bis[5-(2-ethylhexyl)thiophen-2-yl]benzo[1,2-b:4,5-b′]difuran (**6**) were synthesized according to literature procedures.[24]

*Compound **2***

A 100 mL flame-dried flask was charged with 2-(tributylstannyl)-4-octylthiophene (4.95 g, 10.0 mmol), 5-bromothiophene-2-carbaldehyde (1.53 g, 8.0 mmol), and anhydrous toluene (35 mL). The mixture was degassed with argon for 30 min. $[Pd(PPh_3)_4]$ (0.23 g, 0.2 mmol) was added. The mixture was slowly heated up to 100°C and stirred at this temperature overnight under an argon atmosphere. Then, water was added, and the mixture was extracted with CH_2Cl_2 (3×). The combined organic layer was dried with anhydrous Na_2SO_4. After removing the solvent under reduced pressure, the crude residue was purified by column chromatography (silica gel, petroleum ether/CH_2Cl_2). Finally, **2** (1.59 g, 65%) was obtained as a light yellow solid. ^{1}H NMR (600 MHz, $CDCl_3$): $\delta = 9.85$ (s, 1H), 7.65 (d, 1H), 7.21 (d, 1H), 7.19 (d, 1H), 6.95 (s, 1H), 2.60 (t, 2H), 1.63 (m, 2H), 1.35–1.25 (m, 10H), 0.88 ppm (t, 3H). ^{13}C NMR (150 MHz, $CDCl_3$): $\delta = 182.53$, 147.68, 144.79, 141.45, 137.35, 135.63, 127.46, 123.91, 121.93, 31.87, 30.40, 30.38, 29.39, 29.27, 29.25, 22.67, 14.11 ppm.

*Compound **3***

N-Bromosuccinimide (NBS; 0.89 g, 5.0 mmol) was added in small portions to a solution of **2** (1.53 g, 5.0 mmol) in $CHCl_3$ (35 mL) and acetic acid (35 mL). In the absence of light, the mixture was stirred for 6 h at room temperature. The mixture was diluted with water and extracted with CH_2Cl_2 (3×). The organic phase was dried with Na_2SO_4. After removing the solvent under reduced pressure, the crude product was purified by column chromatography (silica gel, petroleum ether/CH_2Cl_2). Compound **3** (1.35 g, 70%) was obtained as a yellow solid. ^{1}H NMR (600 MHz, $CDCl_3$): $\delta = 9.84$ (s, 1H), 7.62 (d, 1H), 7.13 (d, 1H), 7.02(s, 1H), 2.53 (t, 2H), 1.58 (m, 2H), 1.33–1.25 (m, 10H), 0.88 ppm (t, 3H). ^{13}C NMR (150 MHz, $CDCl_3$): $\delta = 182.37$, 146.25, 143.66, 141.72, 137.22, 135.39, 126.75, 124.03, 110.96, 31.86, 29.60, 29.52, 29.34, 29.22, 29.20, 22.67, 14.12 ppm.

*Compound **4***

A 50 mL flame-dried flask was charged with **3** (1.15 g, 3.0 mmol), 2-(tributylstannyl)-4-octylthiophene (1.58 g, 3.25 mmol), and anhydrous toluene (20 mL). The mixture was degassed with argon for 30 min. $[Pd(PPh_3)_4]$ (91 mg, 0.08 mmol) was added quickly. The mixture was slowly heated up to 100°C and stirred at this temperature for 12 h under an argon atmosphere. Then, the cooled mixture was poured into water and extracted with CH_2Cl_2 (3×). The combined organic layer was dried with anhydrous Na_2SO_4. After removing the solvent under reduced pressure, the crude residue was purified by column chromatography (silica gel, petroleum ether/CH_2Cl_2). Compound **4** (0.9 g, 60%) was obtained as a red solid. ^{1}H NMR (600 MHz, $CDCl_3$): $\delta = 9.84$ (s, 1H), 7.64 (d, 1H), 7.19 (d, 1H), 7.17 (s, 1H), 6.99 (d, 1H), 6.93 (s, 1H), 2.73 (t, 2H), 2.60 (t, 2H), 1.67–1.61 (m, 4H), 1.40–1.27 (m, 20H), 0.88 ppm (m, 6H). ^{13}C NMR (150 MHz, $CDCl_3$): $\delta = 182.39$, 147.15, 143.87, 141.40, 140.51, 137.40, 134.84, 133.28, 133.11, 129.00, 127.75, 123.85, 120.79, 31.90, 31.88, 30.50, 30.46, 30.43, 29.52, 29.44, 29.38, 29.34, 29.30, 29.28, 29.26, 22.68, 14.12 ppm.

*Compound **5***

NBS (0.27 g, 1.51 mmol) was added in small portions to a solution of **4** (0.75 g, 1.5 mmol) in $CHCl_3$ (25 mL) and acetic acid (25 mL). In the absence of light, the mixture was stirred for 6 h at room temperature. The mixture was diluted with water and extracted with CH_2Cl_2 (3×). The organic phase was dried with Na_2SO_4. After removing the solvent under reduced pressure, the crude product was purified by column chromatography (silica gel, petroleum ether/CH_2Cl_2). Compound **5** (0.69 g, 80%) was obtained as an orange solid. ^{1}H NMR (600 MHz, $CDCl_3$): $\delta = 9.86$ (s, 1H), 7.66 (d, 1H), 7.21 (d, 1H), 7.16 (s, 1H), 6.85 (s, 1H), 2.70 (t, 2H), 2.57 (t, 2H), 1.66–1.58 (m, 4H), 1.38–1.25 (m, 20H), 0.89 ppm (m, 6H). ^{13}C NMR (150 MHz, $CDCl_3$): $\delta = 182.39$, 146.80, 142.69, 141.63, 141.03, 137.34, 134.65, 133.63, 132.12, 128.91, 127.23, 124.04, 109.57, 31.89, 31.87, 30.50, 29.67, 29.53, 29.47, 29.38, 29.37, 29.28, 29.25, 22.68, 14.13 ppm. MS (UHR-TOF): *m*/*z*: calcd for $C_{29}H_{39}BrOS_3$: 578.1346 [M^+]; found: 578.1342. Elemental analysis calcd (%) for $C_{29}H_{39}BrOS_3$ (579.72): C 60.08, H 6.78, S 16.59; found: C 59.95, H 6.75, S 16.38.

Compound **7**

A three-necked 50 mL flask was charged with **5** (0.58 g, 1.0 mmol), **6** (0.39 g, 0.45 mmol), and anhydrous toluene (20 mL). The mixture was degassed with argon (3×). $[Pd(PPh_3)_4]$ (46 mg, 0.04 mmol) was added quickly under an argon atmosphere. The mixture was slowly heated up to 100 °C and stirred at this temperature for 36 h under an argon atmosphere. Then, the cooled mixture was poured into water and extracted with CH_2Cl_2 (3×). The combined organic layer was dried with Na_2SO_4. After removing the solvent under reduced pressure, the crude residue was purified by column chromatography (silica gel, petroleum ether/CH_2Cl_2). Compound **7** (0.42 g, 60%) was obtained as a red solid. ^{1}H NMR (600 MHz, $CDCl_3$): $\delta = 9.86$ (s, 2H), 7.78 (s, 2H), 7.66 (d, 2H), 7.44 (d, 2H), 7.23 (d, 2H), 7.20 (s, 2H), 7.05 (s, 2H), 6.94 (d, 2H), 2.99 (t, 2H), 2.90 (dd, 2H), 2.83 (t, 2H), 1.81–1.69 (m, 10H), 1.38–1.26 (m, 56H), 0.98–0.85 ppm (m, 24H). ^{13}C NMR (150 MHz, $CDCl_3$): $\delta = 182.39$, 151.23, 147.95, 146.91, 144.91, 141.67, 141.50, 141.02, 137.40, 134.55, 134.15, 133.04, 132.70, 129.31, 129.20, 127.57, 127.47, 125.76, 124.85, 123.96, 109.09, 103.58, 41.53, 34.23, 32.54, 31.96, 31.92, 30.42, 30.08, 29.90, 29.83, 29.71, 29.63, 29.49, 29.42, 29.33, 28.98, 25.59, 23.09, 22.73, 22.70, 14.20, 14.13, 14.12, 10.91 ppm. MS (UHR-TOF): *m*/*z*: calcd for $C_{92}H_{118}O_4S_8$: 1542.6796 [M^+]; found: 1542.6869.

DCA3TBDF

Under protection of argon, octyl cyanoacetate (0.8 mL, 3.8 mmol) was added by syringe to a stirred solution of **7** (0.38 g, 0.25 mmol) in $CHCl_3$ (30 mL) and triethylamine (0.08 mL). The mixture was stirred for 40 h at room temperature under an argon atmosphere. Then, it was poured into water (40 mL) and extracted with $CHCl_3$ (3×). The organic phase was dried with Na_2SO_4. After removing the solvent under reduced pressure, the crude product was purified by column chromatography (silica gel, petroleum ether/CH_2Cl_2). DCA3TBDF (0.38 g, 80%) was obtained as a black solid. ^{1}H NMR (600 MHz, $CDCl_3$): $\delta = 8.21$ (s, 2H), 7.78 (d, 2H), 7.60 (d, 2H), 7.39 (s, 2H), 7.20 (s, 2H), 7.17 (d, 2H), 7.01 (s, 2H), 6.95 (d, 2H), 4.27 (t, 4H), 2.95 (t, 4H), 2.91 (t, 4H), 2.80 (t, 4H), 1.74 (m, 14H), 1.52–1.29 (m, 76H), 0.98 (t, 6H), 0.94–0.86 ppm (m, 24H). MS (UHR-TOF): *m*/*z*: calcd for $C_{114}H_{152}N_2O_6S_8$: 1900.9416 [M^+]: found: 1900.9489. Elemental analysis calcd (%) for $C_{114}H_{152}N_2O_6S_8$ (1902.96): C 71.95, H 8.05, N 1.47, S 13.48; found: C 72.01, H 8.03, N 1.43, S 13.42.

Acknowledgements

This work was supported by the Ministry of Science and Technology of China (2014CB643501, 2010DFA52310), National Natural Science Foundation of China (21274161, 21202181, 51173199, 51211140346), and Shandong Provincial Natural Science Foundation (ZR2011BZ007).

[1] G. Yu, J. Gao, J. C. Hummelen, F. Wudl, A. J. Heeger, *Science* **1995**, *270*, 1789–1791.
[2] J. W. Chen, Y. Cao, *Acc. Chem. Res.* **2009**, *42*, 1709–1718.
[3] B. C. Thompson, J. M. Fréchet, *Angew. Chem. Int. Ed.* **2008**, *47*, 58–77; *Angew. Chem.* **2008**, *120*, 62–82.
[4] J. H. Hou, H. Y. Chen, S. Q. Zhang, R. I. Chen, Y. Yang, Y. Wu, G. Li, *J. Am. Chem. Soc.* **2009**, *131*, 15586–15587.
[5] H. Zhou, L. Yang, W. You, *Macromolecules* **2012**, *45*, 607–632.
[6] Z. He, C. Zhong, S. Su, M. Xu, H. Wu, Y. Cao, *Nat. Photonics* **2012**, *6*, 591–595.
[7] Y. Liu, Y. M. Yang, C. C. Chen, Q. Chen, L. Dou, Z. Hong, G. Li, Y. Yang, *Adv. Mater.* **2013**, *25*, 4657–4662.
[8] D. H. Wang, A. K. K. Kyaw, V. Gupta, G. C. Bazan, A. J. Heeger, *Adv. Energy Mater.* **2013**, *3*, 1161–1165.
[9] C. Cui, J. Min, C. L. Ho, T. Ameri, P. Yang, J. Zhao, C. J. Brabec, W. Y. Wong, *Chem. Commun.* **2013**, *49*, 4409–4411.
[10] S. Loser, C. J. Bruns, H. Miyauchi, R. P. Ortiz, A. Facchetti, S. I. Stupp, T. J. Marks, *J. Am. Chem. Soc.* **2011**, *133*, 8142–8145.
[11] J. Liu, Y. Sun, P. Moonsin, M. Kuik, C. M. Proctor, J. Lin, B. B. Hsu, V. Promarak, A. J. Heeger, T. Q. Nguyen, *Adv. Mater.* **2013**, *25*, 5898–5903.
[12] J. Zhou, Y. Zuo, X. Wan, G. Long, Q. Zhang, W. Ni, Y. Liu, Z. Li, G. He, C. Li, B. Kan, M. Li, Y. Chen, *J. Am. Chem. Soc.* **2013**, *135*, 8484–8487.
[13] A. Tang, L. Li, Z. Lu, J. Huang, H. Jia, C. Zhan, Z. Tan, Y. Li, J. Yao, *J. Mater. Chem. A* **2013**, *1*, 5747–5757.
[14] C. Cabanetos, A. El Labban, J. A. Bartelt, J. D. Douglas, W. R. Mateker, J. M. Fréchet, M. D. McGehee, P. M. Beaujuge, *J. Am. Chem. Soc.* **2013**, *135*, 4656–4659.
[15] L. Huo, S. Zhang, X. Guo, F. Xu, Y. Li, J. Hou, *Angew. Chem. Int. Ed.* **2011**, *50*, 9697–9702; *Angew. Chem.* **2011**, *123*, 9871–9876.
[16] J. Min, Z.-G. Zhang, S. Zhang, Y. Li, *Chem. Mater.* **2012**, *24*, 3247–3254.
[17] Y. Lin, L. Ma, Y. Li, Y. Liu, D. Zhu, X. Zhan, *Adv. Energy Mater.* **2013**, *3*, 1166–1170.
[18] Y. Liu, X. Wan, F. Wang, J. Zhou, G. Long, J. Tian, Y. Chen, *Adv. Mater.* **2011**, *23*, 5387–5391.
[19] B. Liu, X. Chen, Y. He, Y. Li, X. Xu, L. Xiao, L. Li, Y. Zou, *J. Mater. Chem. A* **2013**, *1*, 570–577.
[20] X. Chen, B. Liu, Y. Zou, L. Xiao, X. Guo, Y. He, Y. Li, *J. Mater. Chem.* **2012**, *22*, 17724–17731.
[21] U. H. Bunz, *Angew. Chem. Int. Ed.* **2010**, *49*, 5037–5040; *Angew. Chem.* **2010**, *122*, 5159–5162.
[22] C. H. Woo, P. M. Beaujuge, T. W. Holcombe, O. P. Lee, J. M. Fréchet, *J. Am. Chem. Soc.* **2010**, *132*, 15547–15549.
[23] O. Gidron, A. Dadvand, Y. Sheynin, M. Bendikov, D. F. Perepichka, *Chem. Commun.* **2011**, *47*, 1976–1978.
[24] L. Huo, L. Ye, Y. Wu, Z. Li, X. Guo, M. Zhang, S. Zhang, J. Hou, *Macromolecules* **2012**, *45*, 6923–6929.
[25] H. Wang, F. Liu, L. Bu, J. Gao, C. Wang, W. Wei, T. P. Russell, *Adv. Mater.* **2013**, *25*, 6519–6525.
[26] S. C. Price, A. C. Stuart, W. You, *Macromolecules* **2010**, *43*, 4609–4612.
[27] W. Guo, S. Wang, K. Sun, M. E. Thompson, S. R. Forrest, *Adv. Energy Mater.* **2011**, *1*, 184–187.
[28] D. Lee, E. Hubijar, G. J. D. Kalaw, J. P. Ferraris, *Chem. Mater.* **2012**, *24*, 2534–2540.
[29] G. G. Malliaras, J. R. Salem, P. J. Brock, C. Scott, *Phys. Rev. B* **1998**, *58*, R13411–R13414.
[30] X. Hu, L. Zuo, W. Fu, T. T. Larsen-Olsen, M. Helgesen, E. Bundgaard, O. Hagemann, M. Shi, F. C. Krebs, H. Chen, *J. Mater. Chem.* **2012**, *22*, 15710.
[31] V. D. Mihailetchi, J. Wildeman, P. W. M. Blom, *Phys. Rev. Lett.* **2005**, *94*, 126602.
[32] J. Liu, H. Choi, J. Y. Kim, C. Bailey, M. Durstock, L. Dai, *Adv. Mater.* **2012**, *24*, 538–542.
[33] A. B. Tamayo, X.-D. Dang, B. Walker, J. Seo, T. Kent, T.-Q. Nguyen, *Appl. Phys. Lett.* **2009**, *94*, 103301.
[34] J. A. Love, C. M. Proctor, J. Liu, C. J. Takacs, A. Sharenko, T. S. van der Poll, A. J. Heeger, G. C. Bazan, T.-Q. Nguyen, *Adv. Funct. Mater.* **2013**, *23*, 5019–5026.

Received: May 2, 2014
Published online: July 13, 2014

